Cell Stem Cell, Volume *3*

Supplemental Data

Hematopoietic Stem Cell Function and Survival Depend on c-Myc and N-Myc Activity

Elisa Laurenti, Barbara Varnum-Finney, Anne Wilson, Isabel Ferrero, William E. Blanco-Bose, Armin Ehninger, Paul S. Knoepfler, Pei-Feng Cheng, H. Robson MacDonald, Robert N. Eisenman, Irwin D. Bernstein, and Andreas Trumpp

SUPPLEMENTAL EXPERIMENTAL PROCEDURES

Mice

All mice were maintained in the ISREC animal facility under specific pathogen free (SPF) conditions and housed in individually ventilated cages (HIVC). Animal procedures were performed according to protocols approved by the Swiss Bundesamt für Veterinärwesen No: 1728.

C57BL/6 ($CD45.2^+$) and B6.SJL-Ptprc(a)Pep(b)BoyCrl(Ly5.1) ($CD45.1^+$) female mice were purchased respectively from Harlan Olac (The Netherlands) and Charles River (l'Arbresle, France).

Flow-cytometry and purification of HSCs

Lin^- BM was prepared by staining with a cocktail of mAbs against the following lineage markers: CD3e (17A2), CD4 (GK1.5), CD8a (53.6.7), CD11b (M1/70), CD19 (1D3), Gr1 (RB6.8C5), Ter119 and NK1.1 (PK136). Labeled cells were then removed by 2 consecutive incubations with anti-Rat IgG-coated M450 Dynabeads (Dynal, Invitrogen) at a 10:1 bead-to-target cell ratio. Lin^- enriched cells were successively stained with Ab

against: CD34 (RAM 34)-FITC and Alexa 647; CD135 (Flt3 A2F10)-PE; CD48 (HM48.1)-FITC and APC; CD117 (ckit 2B8)-PE, PE-Cy5, PE-Cy7, APC and APCAlexa750; Sca1 (D7)-PE-Cy5, PE-Cy7, APC and biotin, CD16/32 (93)-PE and Pacific blue. For analysis of mature differentiated cell types, total BM cells were stained with anti-CD11b (M1/70)-PE, PECy5 and PECy7, Gr1 (RB6.8C5)-PE, PECy7, Alexa647 and APCAlexa750, CD3e (17A2)-FITC, CD4 (GK1.5)-FITC and PECy7, CD8a (53.6.7)-FITC and PECy7, CD161 (PK136)-FITC and biotin, CD49b (DX5)-FITC, PECy7 and biotin, B220 (RA3-6B2)-PECy7 and APC, CD19 (6D5)-PeCy5, CD43 (R2/60)-FITC or biotin, CD93 (AA4.1)-APC, IgMtot (II/41)-PE, CD41-FITC or PE, Ter119-FITC, PECy7 and APCAlexa750, CD45.1 (A20)-FITC and PECy7, and CD45.2 (104)-PECy5.5, Pacific Blue, Alexa647 and biotin antibodies. StreptAvidin conjugate used were APC-Alexa750 and PacificBlue. All monoclonal antibody conjugates were purchased from eBiosciences (except CD150 from BioLegend) or purified and conjugated in our laboratory according to standard protocols. Cell sorting was performed on a FACS Vantage™ or a FACS Aria™ Flow Cytometer (Becton Dickinson, San Jose, CA). 4 to 6 colors FACS analysis was performed on a FACS Canto™ instrument (Becton Dickinson), while 7 to 9 colours and cell cycle analyses were carried out on a CyAn™ ADP (DAKO, Glostrup, Denmark). Data was analysed with FlowJo software (Tree Star, Ashland, OR).

Limiting dilution BM transplantation

To assess competitive repopulation frequencies of $Nmyc^{fl/fl}Cre^{+}$ or $Nmyc^{fl/fl}Cre^{-}$, we injected 5-groups of lethally irradiated recipients (4-6-recipients per group in two

separate experiments) with limiting dilutions of *Nmyc*$^{fl/fl}$*Cre*$^{+}$ or *Nmyc*$^{fl/fl}$*Cre*$^{-}$ LSK donor cells (CD45.2^{+}). Test cells were injected intravenously via the tail vein along with 1 x 10^5 freshly isolated, unseparated recipient (CD45.1^{+}) bone marrow cells as competitors. We considered an animal positive for engraftment if there were $\geq$ 2% viable, CD45.2^{+} donor cells of the myeloid, T and B cell lineages in peripheral blood of recipients more than 9-weeks after the transplant. We calculated the frequency of LT-HSC from the proportions of negative or non-engrafted mice within each experimental group using the method of maximum likelihood using the L-CALC software (StemCell Technologies, Vancouver, BC, Canada).

Microarray analysis

For microarray analysis, RNA was extracted from Lin^{-} Sca1^{+} CD150^{+} CD48^{-} (LT-HSCs) and Lin^{-} Sca1^{+} CD150^{+} CD48^{+} (committed progenitors) cells sorted 4 days after the first pIpC injection. Each condition was analysed in triplicates, with each replicate consisting of a pool of 3 dKO mice or 2 control mice. Two rounds of amplification for each RNA sample were performed utilizing the Nugen WT-Ovation Pico RNA Amplification System (Nugen, San Carlos, CA, USA). Biotin labelling of cRNA was performed utilizing the Affymetrix GeneChip IVT labelling kit (Affymetrix, Santa Clara, CA, USA). This biotinylated RNA was fragmented and hybridized to Affymetrix MOE430v.2 chips (Affymetrix, Santa Clara, CA, USA) as per the manufacturers protocol. Both raw image (.dat) and intensity (.cel) files were generated utilizing the Affymetrix Gene Chip Operating Software (GCOS).

Quality control tests were performed utilizing the DNA Array Facility of Lausanne's Remote Analysis System (http://race.unil.ch). This is a web-based interface for various

statistical analysis routines performed utilizing the R language (http://www.r-project.org). These involved various quality tests such as the comparison of RNA 5' end to 3'end bias utilizing RNA degradation plots to determine the quality of amplification; density of PM intensities; RMA normalization of the chips; sample clustering to control replicates; correlation matrix to observe correlation between samples and replicates; surface intensity in log scale to examine for chip and hybridization defects; scatter plots to compare samples and replicates. Chips that did not fit these quality checks were eliminated from the sample and not considered in the following statistical analysis. RMA normalized data was entered into the Genespring program (Silicon Genetics) for data visualization as well as further filtering and examination of overlaps of various gene lists. Samples having passed the quality check were then further statistically analysed using the Statistical Bayes Test Module on the RACE system. Genes showing a 2-fold difference with a minimum Baysian p value of 0.05 were then selected. These genes were then further analysed for significant genes and pathways using Ingenuity Pathways Analysis (Ingenuity Systems, Redwood City, CA, USA).

RT-PCR

For Real-time PCR, total RNA was reverse-transcribed using random nonamers and AMV reverse transcriptase (Roche). For the PCR reaction, the LightCycler-FastStart DNA Master SYBR Green I (Roche) was used on a LightCycler instrument (Roche) following the instruction manual. The primers used for RT-PCR were the following: *c-myc*: forward: GGA CAG TGT TCT CTG CC, reverse: CGT CGC AGA TGA AAT AGG; or forward: CAC CAG CAG CGA CTC TGA, reverse: GGG GTT TGC CTC TTC TCC; *N-myc*: forward: TGC CGA ATG TGT GGA C, reverse: CGC ACA GTG ATC

GTG AA; or forward: CTC CGG AGA GGA TAC CTT GA, reverse: TCT CTA CGG TGA CCA CAT CG; *L-myc*: forward: CGG CAC TCC TAG TCT G, reverse: GCT GCT GTT GGT GGA TA; *TBP*: forward: CCT TCA CCA ATG ACT CCT ATG AC, reverse: CAA GTT TAC AGC CAA GAT TCA C. *GrA*, *GrB*, *GrC* and *Spi-6* primers were previously described (Revell et al., 2005; Zhang et al., 2006). Amplification plots were analysed using the second derivative method with LC data analysis 3.5 software (Roche) and the relative quantification was determined using the LightCycler relative quantification software 1.0 (Roche). Triplet analysis showed that measurement errors were always < 5%.

Optimization of the absolute quantification of *c-myc* and *N-myc* transcripts

c-myc, *N-myc* and *L-myc* cDNAs, flanked by restriction sites, were PCR-amplified from total cDNA of E11 embryos using Advantage Polymerase (Clontech) and inserted into the TOPO cloning vector pCRII (Invitrogen). Following sequence verification, the cDNAs were digested and gel purified (Jetquick gel spin kit, Genomed). The concentrations (in ng/μL) were determined using a Nanodrop spectrophotometer (Thermo Scientific). The measured concentrations were converted into molar concentrations based on the molecular weight. Standard curves using known molar amounts of purified *c-myc*, *N-myc* and *L-myc* cDNA were run on the Light Cycler to determine the factor necessary to compare the amounts of *c-myc* and *N-myc* measured by qRT-PCR with the same primers. Consequently, the values for *N-myc* need to be multiplied by the factor 1.29 to be comparable to the *c-myc* values, while *L-myc* values have to be divided by 1.44 for direct comparison to *c-myc*.

TUNEL/GrB double staining by FACS:

After lineage depletion and staining for appropriate cell surface markers, cells were fixed for 30mn in 2% PFA, permeabilized for 2 min in 0.1% Triton X-100 in 0.1% NaCitrate and then labeled for TUNEL according to the *in situ* cell death detection kit (Roche) instructions. The cells were then incubated overnight with GrB antibody.

***In vitro* deletion with IFNα**

After depletion of lineage positive cells as described above, $5x10^2$- $5x10^3$ or $2.5x10^5$ were plated respectively in 96 well-dishes or 24 well-dishes in Stem Pro-34SFM medium (GIBCO Invitrogen Corp.) supplemented with L-glutamine (2mM, GIBCO), Pen/Strep (100 U/mL, GIBCO), mSCF (50 ng/mL), mTPO (25 ng/mL), mFlt3L (30 ng/mL), and IL-11 (10^5 U/mL) all purchased from R&D (Research Diagnostics Inc.). IFNα was then added to the wells (1500 U/mL). The cells were harvested at the indicated time points and stained with a combination of markers and either AnnexinV/7AAD or icGrB as described above.

Activated NK/CTLs isolation:

Spleens from C57/Bl6 mice were collected 24 hours after pIpC injection (5μg/g mouse). Spleen single cell suspensions were enriched for CD8+ and/or Dx5+ via MACS Positive Biotin Bead Selection (Miltenyi Biotech), according to the manufacturing protocol.

SUPPLEMENTAL REFERENCES

Revell, P.A., Grossman, W.J., Thomas, D.A., Cao, X., Behl, R., Ratner, J.A., Lu, Z.H., and Ley, T.J. (2005). Granzyme B and the downstream granzymes C and/or F are important for cytotoxic lymphocyte functions. J Immunol *174*, 2124-2131.

Zhang, M., Park, S.M., Wang, Y., Shah, R., Liu, N., Murmann, A.E., Wang, C.R., Peter, M.E., and Ashton-Rickardt, P.G. (2006). Serine protease inhibitor 6 protects cytotoxic T cells from self-inflicted injury by ensuring the integrity of cytotoxic granules. Immunity *24*, 451-461.

SUPPLEMENTAL FIGURE LEGENDS

FIGURE S1

***N-myc or c-myc* and *N-myc* are efficiently downregulated after pIpC treatment.**

A) Quantification of the levels of *c-myc*, *N-myc* and *L-myc* mRNA by q-RT-PCR in sorted LSK (days 7 and 26) or LSK-SP (day 11) cells from *N-myc flox*^{2} (±MxCre) mice at the indicated time points after pIpC injection. At least 2 mice of each genotype were pooled at each time point.

B-C) Quantification of the levels of *c-myc*, *N-myc* and *L-myc* mRNA by q-RT-PCR in Lin$^-$ cells from *c-myc flox*^{2} *N-myc flox*^{2} (±MxCre) 4 days after the first pIpC injection (B) or in a competitive transplantation setting, CD45.1-2 (MxCre$^+$) Lin$^-$ Sca1$^+$ FACS sorted cells (C). TBP was used to normalize for equal input of RNA. Data in A) represent mean ± SD from a total of 3 control and 5 dKO animals. In B), *c-myc* and *N-myc* transcripts were significantly downregulated ($p<0.0001$) but *L-myc* levels were not changed ($p>0.1$).

FIGURE S2

Kinetics of differentiated cell types numbers in major hematopoietic organs.

(A,B) Absolute numbers of myeloid ($Gr1^+$ $CD11b^+$), early erythroblasts ($Ter119^+$ $CD71^+$), lymphoid cells ($B220^+$) compared to control mice in the bone marrow (A) and in the spleen (B).

C) Electrooptical platelets counts in peripheral blood performed with a Sysmex XE-2100 instrument.

D) Absolute numbers of SLAM HSCs (Lin^- $Sca1^+$ $CD150^+$ $CD48^-$) in the spleen relative to controls. Data represent mean ± SD of at least 3 mice per genotype.

FIGURE S3

dKO hematopoietic progenitors display enhanced apoptosis *in vitro*.

Lin^- progenitors were harvested from *c-myc*$^{flox/flox}$ *N-myc*$^{flox/flox}$ *(±MxCre*) mice, 2000 cells/well were plated in 96-well dishes and incubated at 37°C in StemPRO medium complemented with SCF, IL-11, mTPO and Flt3, in the presence or in the absence of 1500U/mL IFNα. Triplicates were plated for each condition. Cells were harvested and stained with Lin, CD117 and Sca1 antibodies, then with AnnexinV-Cy5 and 7-AAD (BD Biosciences) according to the manufacturer's protocol at the indicated time points. Deletion of both *c-myc* and *N-myc* was observed in $MxCre^+$ wells as soon as 24h after IFNalpha addition (data not shown). From 48 hours onwards, significantly more dying ($AnnexinV^+$ $7AAD^-$) LSK were observed among dKO cells than among control ones ($p=0.002$ at 48h and $p=0.010$ at 72h).

FIGURE S4

Non-competititive transplantation experiments demonstrate that *myc*-deletion induced bone marrow failure is hematopoietic autonomous.

A) Transplantation setup: lethally irradiated CD45.1 mice were reconstituted with 100% not yet deleted *MxCre*$^{-}$ or *MxCre*$^{+}$ *c-myc*$^{flox/flox}$ *N-myc*$^{flox/flox}$ CD45.2 bone marrow cells. After stable engraftment (9 weeks), these mice were treated with pIpC and their BM was analysed 14 days later.

B) Total BM cell counts. Mean ± SD is represented (n=2 per genotype).

C) Representative FACS plots from BM cells gated on the Lin^{-} compartment. While a LSK compartment is clearly present in control mice, no LSK were observed in mice transplanted with MxCre^{+} cells.

D) Representative FACS plots of the granulocytic population in control and dKO mice.

FIGURE S5

Proliferation and apoptosis defects seen in Myc-deficient differentiated cell types are cell-autonomous.

A) Proliferation capacity was assessed by administering BrdU to mixed chimeras for 15h before analysis (14 days after pIpC). Percent BrdU^{+} is shown for all major bone marrow terminally differentiated cell types.

B) Apoptosis rates in Gr1^{+} CD11b^{+} cells relative to control, assayed by TUNEL FACS staining in mixed chimeras 14 days after deletion.

Mean ± SD is shown; n=3 for each genotype (* $p<0.1$; *** $p<0.01$).

FIGURE S6

Genetic controls for c-Myc and N-Myc immunofluorescence detection.

Cytospins of Lin^- from control and dKO animals 4 days after pIpC injection. The slides were stained with either c-Myc (N-262,Santa Cruz) rabbit antibody (top panels) or N-Myc (C-19, Santa Cruz) rabbit antibody (bottom panels). Secondary staining was performed with goat anti-rabbit Alexa568. The slides were mounted in DABCO medium and imaged on an Zeiss Axioplan microscope.

FIGURE S7

Expression of GrB-pathway genes in dKO HSCs.

A) qRT-PCR quantification of the levels of mRNA expression of *GrB* (middle), *GrA* (left) and *Spi-6* genes (right) in control (blue) and dKO (red) Lin- Sca1+ CD150+ CD48- HSCs. TBP was used to normalize for equal input of RNA. Data represent mean ± SD from a total of 3 control and 3 dKO samples. *GrA* and *Spi-6* transcripts were not significantly changed upon *c-myc* and *N-myc* deletion ($p=0.44$ and $p=0.99$). In contrast, a 130-fold upregulation of *GrB* levels was observed ($p<0.0001$), consistent with the microarray estimation. Similarly, *GrC* levels were also assessed and could be detected in dKO cells, but not in control cells, confirming the GrC upregulation observed in the microarray.

B) Quantification of the proportions of GrB+ cells that display either a punctuate or a diffuse pattern of GrB protein as detected by immunofluorescence. A minimum of 360 cells were counted from at least 2 slides of Dx5+ CD8+ enriched cell preparations

(positive control), control or dKO Lin- cells. For each condition, slides from 2 independent experiments were analyzed. No GrB+ cells were found in control Lin- slides. Among GrB+ cells (>60 cells/slide), GrB intracellular distribution was blindly scored by analyzing a minimum of 60 GrB+ cells. Each cell was assigned to either the punctuate or diffuse pattern as exemplified in Fig 6H (top right panel: punctuate; bottom panels: diffuse).

SUPPLEMENTAL TABLES

Table S1: cell surface markers phenotypes used within this study

Population name	Cell surface phenotype
LSK	Lin- $Sca1^+$ $cKit^+$
LT-HSCs $CD34^-$	LSK $CD150^+$ $CD48^-$ $CD34^-$
LT-HSCs $CD34^+$	LSK $CD150^+$ $CD48^-$ $CD34^+$
SLAM HSCs	Lin^- $Sca1^+$ $CD150^+$ $CD48^-$
ST-HSCs	LSK $CD150^+$ $CD48^+$ $CD34^+$ $CD135^-$
MPPs	LSK $CD150^-$ $CD48^+$ $CD34^+$ $CD135^-$
LMPPs	LSK $CD150^-$ $CD48^+$ $CD34^+$ $CD135^+$
MEPs	Lin^- $Sca1^-$ $CD117^+$ $CD34^-$ $FcR\gamma^-$
GMPs	Lin^- $Sca1^-$ $CD117^+$ $CD34^+$ $FcR\gamma^+$
CMPs	Lin^- $Sca1^-$ $CD117^+$ $CD34^+$ $FcR\gamma^-$
CLPs	Lin^- Sca1 low CD117 low $CD127^+$ $CD135^+$
Lin^-	$Gr1^-$ $CD11b^-$ $B220^-$ $CD3^-$ $CD4^-$ $CD8^-$ $Ter119^-$ $Dx5^-$ $NK1.1^-$
Granulocytes	$Gr1^+$ $CD11b^+$
Megakaryocytes	$CD41^+$
Erythroblasts	$CD71^+$ $Ter119^+$
Orthochromatic erythroblasts/RBCs	$CD71^+$ $Ter119^-$
B cells	$B220^+$
Pre-ProB	$B220^+$ $CD43^+$ $CD19^-$
ProB	$B220^+$ $CD43^+$ $CD19^+$
PreB	$B220^+$ $CD43^-$ $AA4.1^+$ $IgMtot^-$
NewB	$B220^+$ $CD43^-$ $AA4.1^+$ $IgMtot^+$
MatureB	$B220^+$ $CD43^-$ $AA4.1^-$ $IgMtot^+$
T cells	$CD3^+$ or $CD4^+$ or $CD8^+$
NK cells	$DX5.5^+$ and/or $NK1.1^+$

Table S2: the frequency of HSCs is similar in N-myc-deficient bone marrow compared to normal BM.

Combined results from two independent experiments.

BM cells injected	$Nmyc^{fl/fl}Cre^{-}$		$Nmyc^{fl/fl}Cre^{+}$	
	Mice with 1.0% myeloid and 1.0% lymphoid donor	# of mice	Mice with 1.0% myeloid and 1.0% lymphoid donor	# of mice
12,500	2	8	4	10
25,000	7	9	7	10
50,000	11	11	7	11
100,000	8	10	8	10
200,000	4	4	4	4
Freq / 10^6 BM cells	34		25	
P value	p=0.3			

Table S3: ribosomal proteins that are significantly downregulated in dKO HSCs.

Ribosomal protein	Fold-change
RBPL22	-3.4
RBPL23	-3.3
RBPL32	-3
RBPL	-2.9
RPL37	-2.8
RPL13	-2.6
RPS19, RPLP1	-2.5
RPS26, RPS5	-2.4
RPS13, Arpb, RPL12, RPS10,	-2.3
RBPL18a, RPL22, RPS24, RPL17, RPS13	-2.2
RPS18, RPSL13a, RPS7	-2.1
RPS15, RPL27a, RPL14, RPS12, RPL37a, RPL22, RPL13a	-2.0

Laurenti et al., Suppl. Fig. 1

A

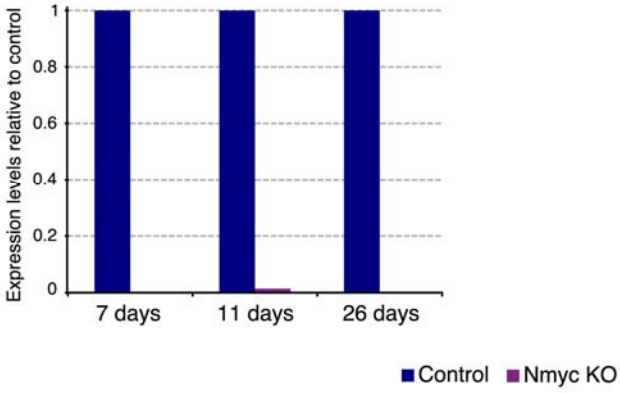

B

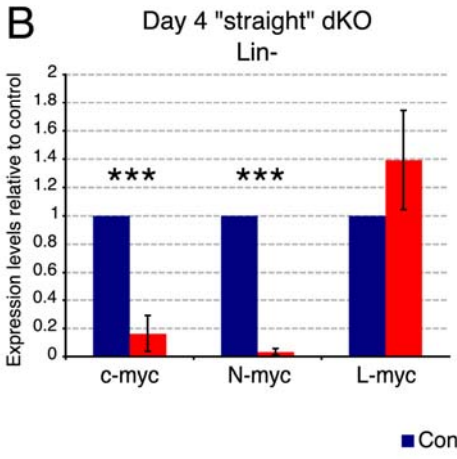

C

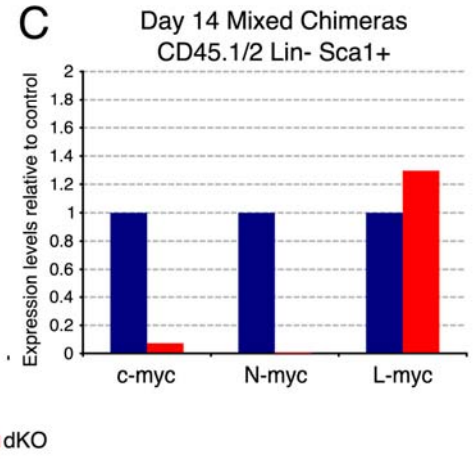

Laurenti et al., Suppl. Fig. 2

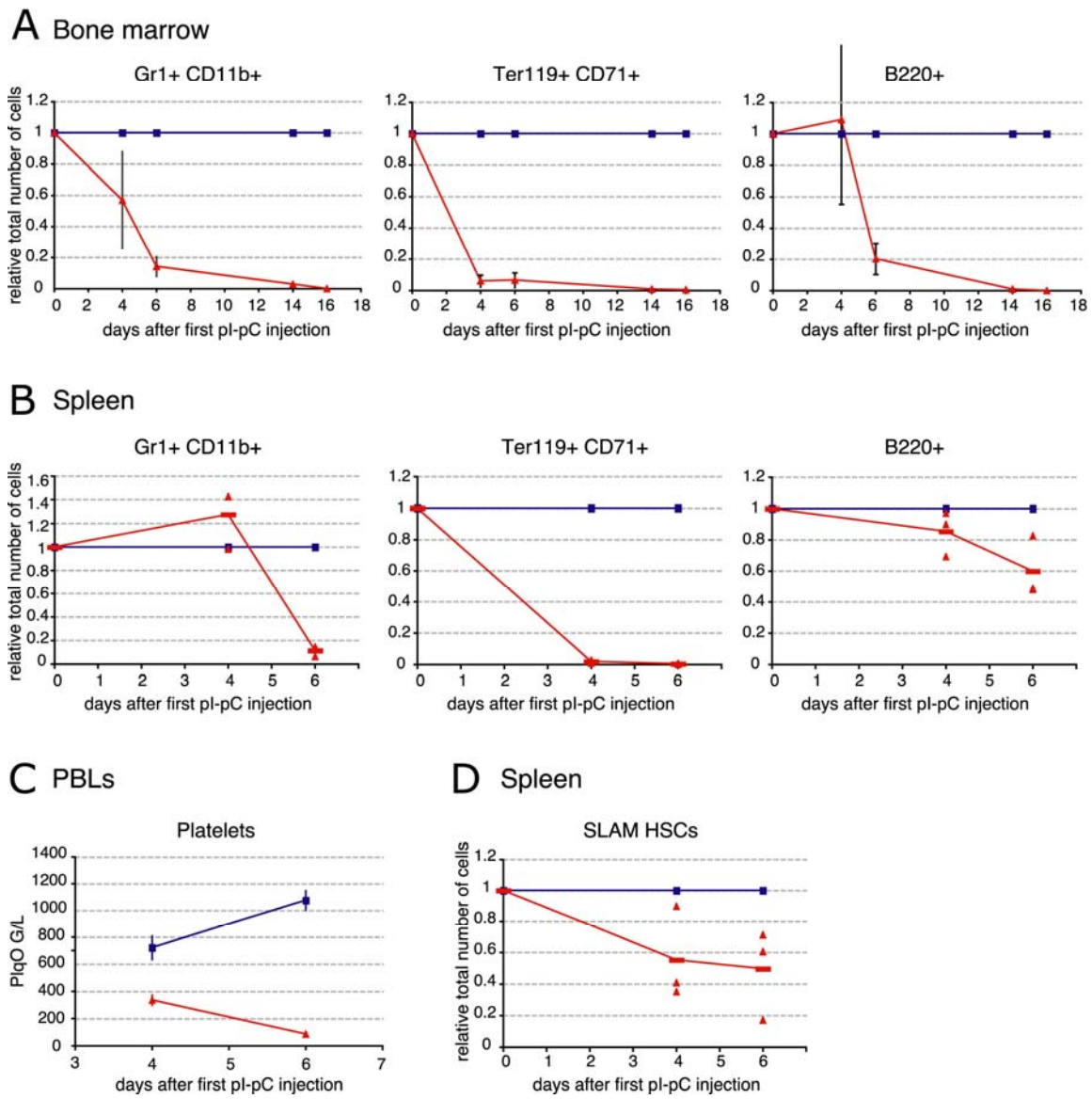

Laurenti et al., Suppl. Fig. 3

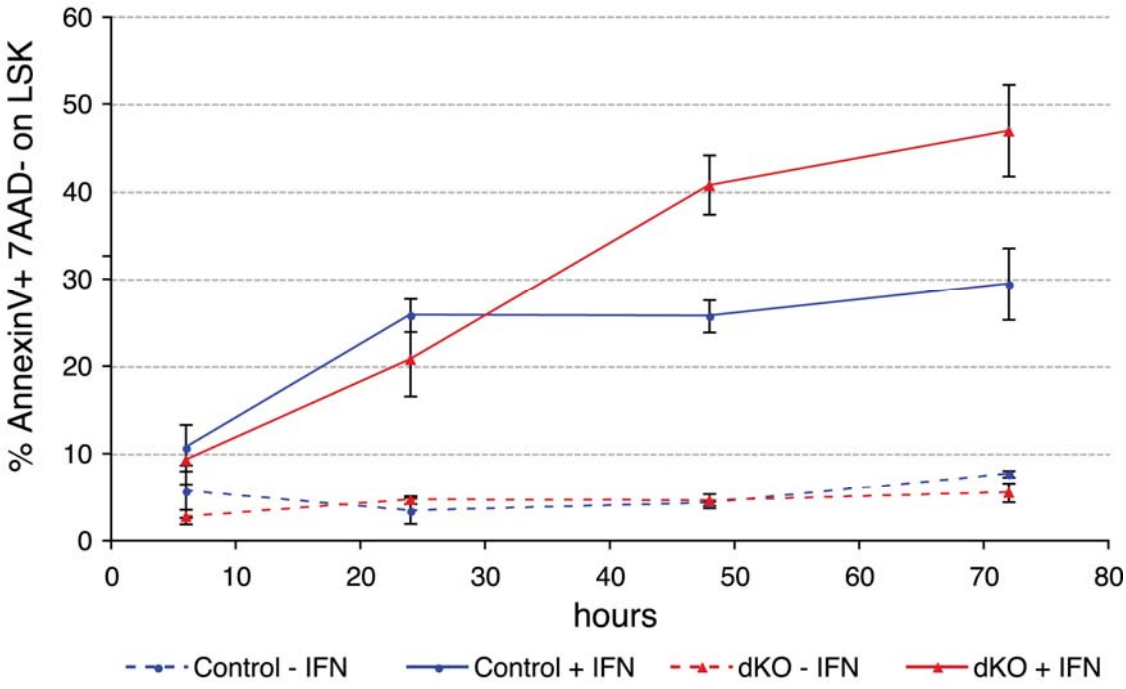

Laurenti et al., Suppl. Fig. 4

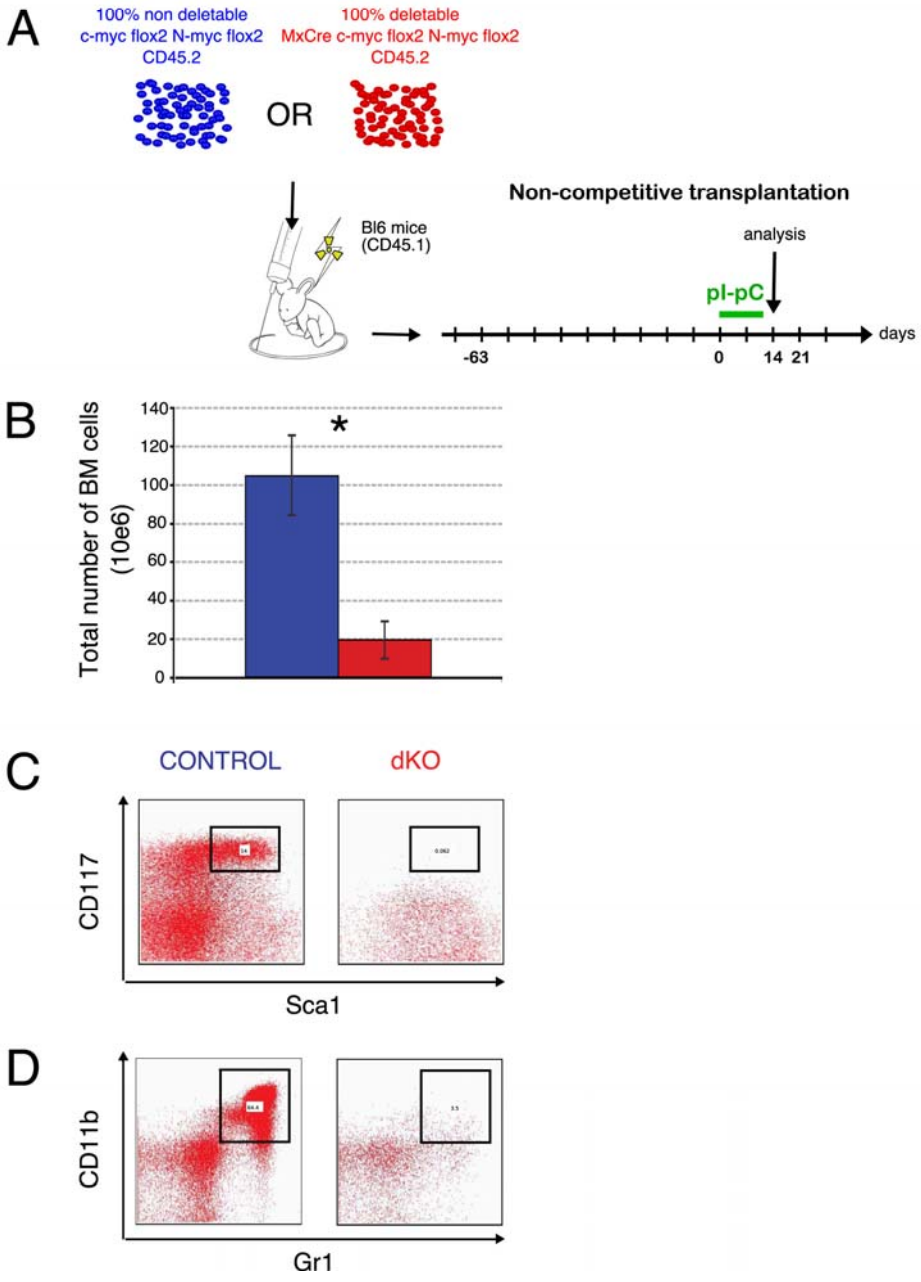

Laurenti et al., Suppl. Fig. 5

A

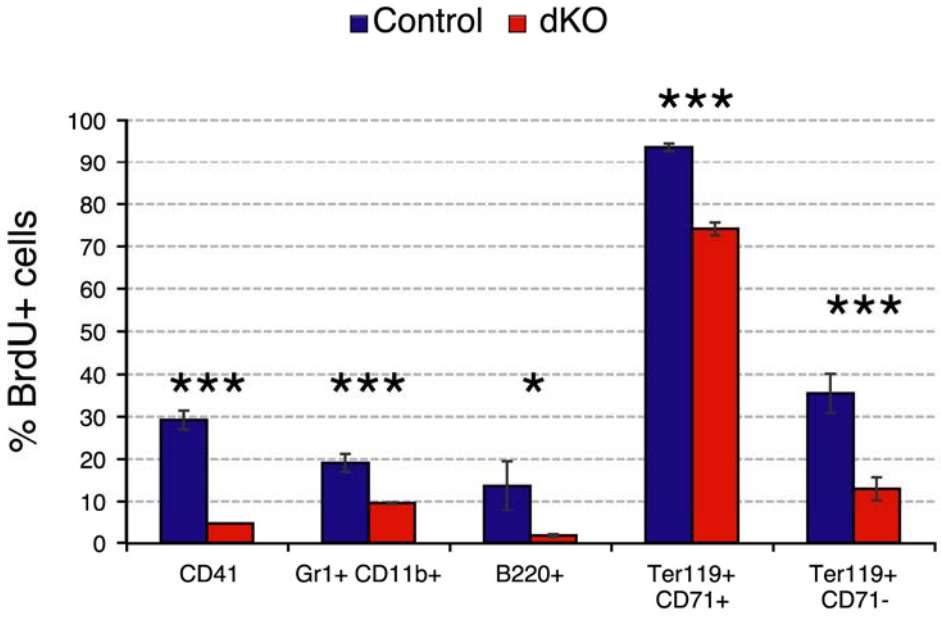

B

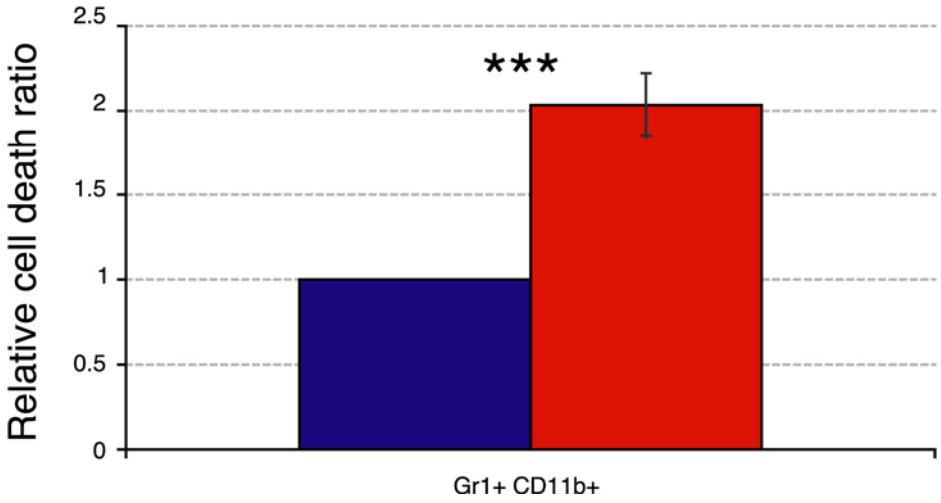

Laurenti et al., Suppl. Fig.6

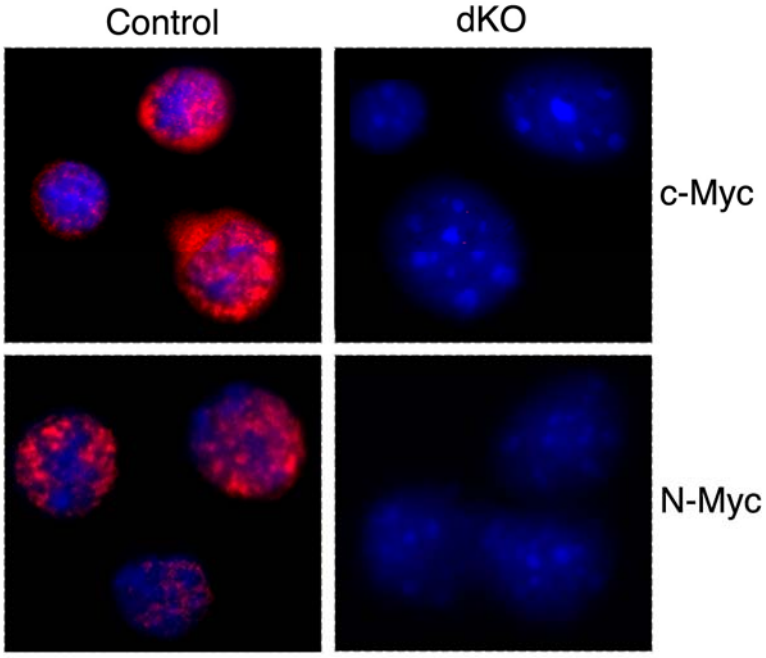

Laurenti et al., Suppl. Fig.7